Enhancing the Command-Following Bandwidth for Transparent Bilateral Teleoperation

Harsimran Singh[1], Aghil Jafari[2], Jee-Hwan Ryu[3], and Angelika Peer[2]

Abstract— **Enhancing transparency of a teleoperation system by increasing the command-following bandwidth has not received lots of attention so far. This is considered a challenging task since in a teleoperation system the command-following bandwidth of the slave robot motion controller cannot be increased with a conventional motion controller as the desired trajectory is instantaneously commanded by the human user and thus, cannot be considered to be given in a pre-computed, smooth second order derivative form. We propose a method to increase the command-following bandwidth by extending the previously introduced Successive Stiffness Increment (SSI) approach to bilateral teleoperation. The approach allows realizing a very high motion controller gain, which cannot be realized with a conventional bilateral teleoperation controller as confirmed by experimental results.**

I. INTRODUCTION

Teleoperation can be considered as one of the oldest fields of robotics and allows a human operator to perform complex manipulation tasks by controlling a remotely located slave robot through interaction with a human interface [1], [2], [3]. Ever since Ray Goertz at the Argonne National Laboratory first proposed a mechanically-driven telerobotic system for handling radioactive material, teleoperation has found its way into different applications. Typical application fields for telerobots include nuclear power plants, space, minimally invasive surgery, and micro/nano manipulation.

Even though many challenges of telerobotic systems have been already addressed in state-of-the-art literature, there still remain unsolved ones. So far teleoperation research e.g. mainly focused on achieving and guaranteeing robust stability under non-ideal communication channels and varying human and remote environment impedances. This includes e.g. the time domain passivity approach (TDPA) proposed to stabilize bilateral teleoperation systems [4], energy bounding algorithms that limit the amount of energy according to the physical damping in the system [5], and absolute stability [6].

However, there has not been much work conducted in terms of improving transparency of teleoperation systems, especially by increasing the command-following bandwidth of motion controllers.

[1]H. Singh is with the Institute of Robotics and Mechatronics in the German Aerospace Center (DLR), 82234 Wessling, Germany. harsimran.singh@dlr.de

[2]A. Jafari and A. Peer are with the University of the West of England, Bristol, United Kingdom. {aghil.jafari,angelika.peer}@uwe.ac.uk

[3]J.H Ryu is with the School of Mechanical Engineering, Korea University of Technology and Education, Cheonan, South Korea. jhryu@koreatech.ac.kr

So far the command-following bandwidth has been mainly determined by the design of the haptic device. Devices with exceptionally low rotor inertia have been developed to render low impedance close to free space. But even with such a haptic device bandwidth mismatches between human and slave robot arm can remain. Attempts to increase the robot's bandwidth by increasing the controller gains typically result in instability. Previous research indicates that standard force control strategies can only achieve stability for low closed-loop bandwidths due to vibratory modes in the robot structure [7], [8], [9]. Having a wider bandwidth of the slave robot close to a human arm (limited to 20 Hz [10]) would not only allow better position tracking capabilities of the slave robot, but also ensure that the user feels as if he/she were moving his/her own arm while actually manipulating a slave robot.

Lots of research has been conducted to improve the command-following behaviour of general robot manipulators. State-of-the-art motion controllers typically consider several derivatives of the to-be-tracked trajectory and allow the robot to follow this trajectory accurately at a reasonably high bandwidth. Derivates are calculated by motion planning algorithms that generally run off-line as the trajectory generation process is computationally expensive. However, in bilateral teleoperation the slave robot motion cannot be pre-planned and depends on the noisy motion command resulting from the interaction of human and master device. Increasing the gain of the motion controller would make the controller stiffer and allow for a better position following behavior of the slave as larger gains improve the bandwidth of the system, but it results in higher overshoot and settling time of the slave robot. Increasing the gain even further, may also compromise stability due to unmodeled structural dynamics. The noisy trajectory of the master can be smoothened using filters, but this would induce a delay in the system. Force feedback renders the closed loop system very sensitive to delay and even small amounts of delay can cause the system to be become unstable. Thus, there is a need for a control framework which increases the bandwidth while maintaining stability during bilateral teleoperation. To the best of the authors knowledge, no research has been conducted into this direction so far.

We approach the problem by extending the previously introduced Successive Stiffness Increment (SSI) approach [11] to bilateral teleoperation. SSI was originally proposed for haptic interaction and allows enlarging the achievable stiffness range by sequentially increasing the rendered feedback force with every interaction cycle resulting in more

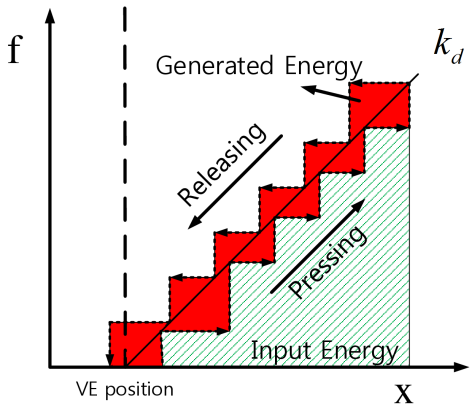

Fig. 1: Position vs. force in single contact haptic interaction.

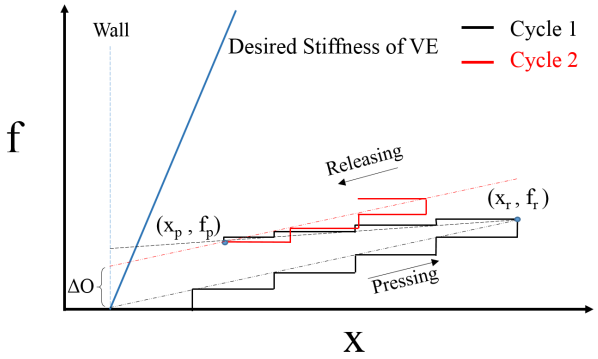

Fig. 2: Basic principle of the SSI approach.

and more pretension of the simulated spring and thus, giving the user the feeling of interacting with an environment that becomes stiffer and stiffer. The interaction cycle has been defined as a set of pressing and releasing paths. We will show that in teleoperation tracking of input and output energy to and from the slave robot allows convergence of the position error between master and slave even for high proportional gains. To implement the approach on a teleoperation system, the pressing and releasing paths had to be identified and an adaptive feedforward force offset added. The extended approach is applicable for both linear and non-linear teleoperation systems. Unlike other approaches, our approach does not degrade the tracking performance for high controller gain and doesn't require the knowledge of system parameters. Experimental results of a teleoperation system with a position-force control architecture and high controller gains are provided to validate the postulated increase of bandwidth and illustrates the effectiveness of the proposed approach.

II. Review of SSI Approach

Recently, the SSI approach was proposed for enlarging the achievable stiffness range of impedance-type haptic displays [11]. The main idea is based on sequentially increasing the force offset to the simulated spring in every contact cycle. This approach allows users having a feeling of interacting with an environment that becomes stiffer and stiffer while maintaining passivity of the overall system. As a result, we were able to achieve significantly higher perceived stiffnesses than with any other conventional method. This Section will briefly review the SSI approach.

As it is well known, discretization is one of the major sources of non-passive behavior. Fig. 1 illustrates position x vs. force f when a human user makes a single contact with a spring-like virtual environment (VE) with stiffness k_v. The solid line indicates the behavior of the ideal VE, and the dashed line the actual behavior of the discrete VE. The position vs. force graph shows a staircase-shaped behavior due to discretization effects. The pressing and releasing paths are defined as when the Haptic Interaction Point (HIP) moves into or out of the VE. The area below the pressing line (dashed green area), can be considered as the injected energy into the VE. The area below the releasing line (solid red plus dashed green area), can be considered as the energy released by the VE. Over one cycle of pressing and releasing, the released energy is larger than the injected energy, meaning that the VE generates energy which represents an active behavior.

If the stiffness of the VE is lower than the critical stiffness, defined in [12] as follows,

$$k_v \leq \frac{2b_m}{\Delta T}. \tag{1}$$

where b_m is the physical damping of the haptic display and ΔT the sampling time, the generated energy will be fully dissipated by the physical damping of the haptic device, therefore the overall interaction would be passive and stable. However, when the stiffness of the VE is higher than the critical stiffness, the generated energy may not be fully dissipated by the physical damping of the device, and therefore the system be potentially unstable.

Fig. 2 shows the graphical representation of the SSI approach where the system input and output variables, namely velocity and feedback force, are power conjugated, i.e. input is related to output and their product is power. Conventionally for stable systems, the feedback force is calculated based on a constant value of stiffness given by (1). Let's assume the VE has a high desired stiffness as shown in Fig. 2. Rather than the feedback force following this high stiffness and making the interaction unstable, one of the power conjugate signals, feedback force, was intentionally increased, starting from a small value, by introducing an offset in each interaction cycle which in turn gradually decreased the other conjugate pair, position displacement, to satisfy energy consistency.

To calculate the feedback force, the pressing and releasing paths were made to follow different slopes. By keeping the value of releasing slope less than the pressing slope for each interaction cycle, the position vs. force graph would follow a zigzag like pattern. This would increase the feedback force while converging the position displacement thereby pushing the graph upwards close to the desired stiffness of the VE.

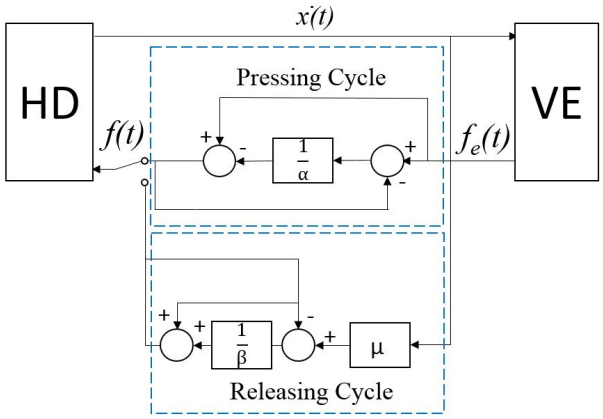

Fig. 3: Control structure of the SSI approach.

Fig. 3 illustrates the control structure of the SSI approach, where it implements two different functions for computing the feedback force for pressing and releasing paths.

The slope for the pressing path depends on (1), whereas the slope for the releasing path is chosen to be less than the one of the pressing path

$$f(k) = f_e(k) - \left(\frac{f_e(k) - f(k-1)}{\alpha} \right) \quad \text{pressing} \quad (2)$$

$$f(k) = f(k-1) + \left(\frac{x(k)\mu - f(k-1)}{\beta} \right) \quad \text{releasing} \quad (3)$$

where $f_e(k) = k_v * x(k)$ is the force of the VE, μ is the displayed stiffness calculated at the end of every pressing path, $x(k)$ is the penetration distance of the HIP inside the VE and α determines the slope of the pressing path. Larger values of α mean a larger slope of the pressing path and vice versa, while β determines the slope of the releasing path.

Fig. 4 shows a comparison in generated energy for the releasing path having equal and less slope than the pressing path. It can be observed that the generated energy is greater when the slope of the releasing path is less than the one of the pressing path as indicated by the shaded region in Fig. 4. If the pressing and releasing path follow (1), then the entire generated energy can be dissipated by the haptic device, keeping the system stable (Fig. 4a). However, if the pressing path follows the slope as indicated in (1), but the releasing path has a slope less than the pressing path, then the energy generated will be greater than what can be dissipated by the haptic device thereby rendering the interaction unstable (Fig. 4b).

To counteract this and as one of the main ideas of the SSI approach, each pressing path is forced to start from the point where the previous releasing path ended thereby introducing an offset (ΔO) that can be considered an added pre-tension to the system. This shifted pressing path injects more energy into the system, which allows compensating the extra energy that was generated by the system at the end of the last cycle.

If the human hand is considered to be passive for the

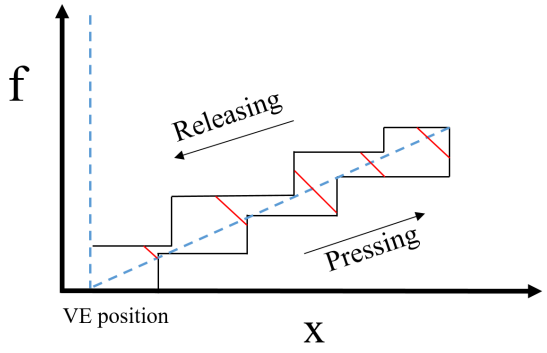

(a)

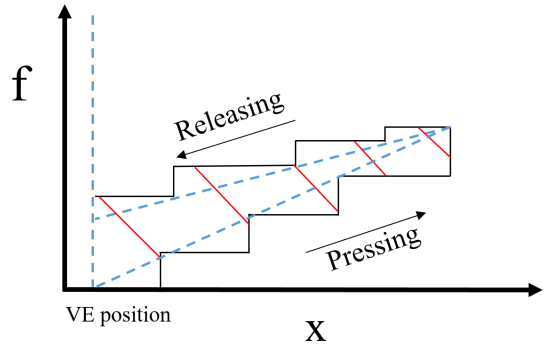

(b)

Fig. 4: (a) Non-changing slope and (b) changing slope for haptic interaction.

frequencies of interest in haptic interaction, during each pressing path, the HIP will penetrate the VE only until the input energy is equal to the output energy of the previous releasing path:

$$output_{k-1} = input_k = \sum_{k=1}^{n} \left[\left(f\left(k-1\right) + \Delta O \right) \Delta x\left(k\right) \right]. \quad (4)$$

Greater the value of ΔO, smaller will be the penetration distance ($\sum_{k=1}^{n} \Delta x\left(k\right)$) for which the input energy ($input_k$) is equal to the output energy ($output_{k-1}$) of the previous releasing path and thus, just keeps the system passive. With each interaction cycle, the penetration distance becomes smaller and the force increases even though the system is generating more energy than can be dissipated by the device. This convergence of penetration distance also reduces the generated energy with each interaction cycle.

III. SSI Approach for Slave Motion Controller

A. Extension of SSI Approach for Motion Controller

The basic principle of the SSI approach is based on intentionally increasing one power conjugate signal (the feedback force from the VE) by introducing an offset in each interaction cycle and allowing to gradually decrease the other conjugate signal (the position displacement) in order to satisfy energy consistency. In order to extend this basic principle to motion controllers, the power conjugate pair which describes the energy input/output relation of

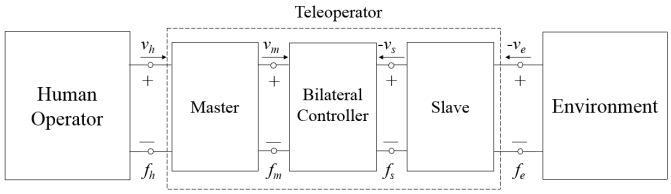

Fig. 5: Block diagram of a complete teleoperation system.

the motion controller (representing the energy exchange as shown in Section II) needs to be identified.

For slave motion control, the difference in position between the master and slave is proportional to the driving force for slave. Therefore, the power conjugate pair that defines the injected and released power is determined by the position error and corresponding slave force. The injected energy is determined via the pressing path whereas the releasing path determines the releasing energy. Fig. 5 shows the block diagram representation for such a network where v_h and v_e are the velocities at the interacting points of the human/master and environment/slave and f_h and f_e are the forces that the user applies to the master manipulator and the slave manipulator applies to the environment. By intentionally altering one of the conjugate pair, it becomes possible to control the other.

As previously illustrated the SSI approach is based on the detection of pressing and releasing paths in haptic interaction, which in turn displays the input and output energy. For a 1-DoF haptic interaction, the pressing and releasing path of the position vs. force graph is always constrained to one quadrant as can be seen in Fig. 1. This is not the case for motion controllers due to the dynamics and control of the slave robot. To apply the SSI approach to slave motion control, it is consequently necessary to determine the injected and released energy to and from the slave robot. If the master is displaced from its equilibrium position, it causes the slave to experience a restoring force proportional to the position error between master and slave. Fig. 6 shows the corresponding position error and force, where the output force is proportional to the position error with gain K_p.

Let's assume that the position error $(x_m - x_s)$ is positive during the first cycle, as shown in Fig. 6. When the user moves the master, the position error increases guiding the slave along the pressing path. The maximum position error for the first cycle is assumed to be bounded with x_1. The area underneath the pressing path constitutes the injected energy to the slave for the first cycle. As soon as the slave tries to follow the master, the error $(x_m - x_s)$ decreases and moves the slave on the releasing path of the first cycle. The area underneath the releasing path is the released energy of the slave (E_{O_1}) during the first cycle.

$$E_{O_1}(n) = \Delta T \sum_{k=0}^{n} K_p(x_m(k) - x_s(k))(\dot{x}_m(k) - \dot{x}_s(k)). \quad (5)$$

As the slave is an energy-dissipative component, some of the generated energy during the first cycle will be dissipated

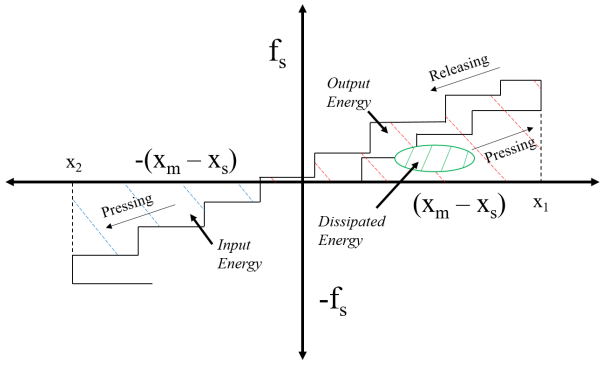

Fig. 6: Graphical illustration of position error vs. slave force.

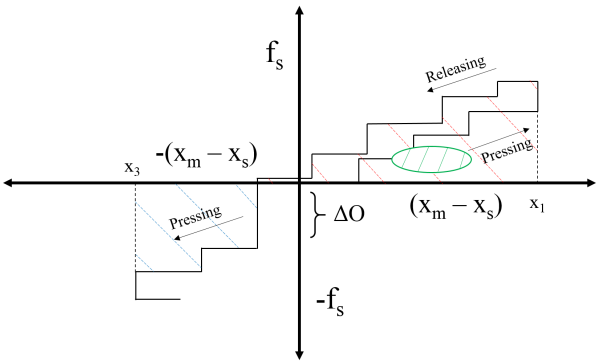

Fig. 7: Graphical illustration of position error vs. feedforward slave force.

by the inherent damping of the device. The slave position then overshoots the master position and moves until the injected energy during the second cycle is equal to the released energy during the first cycle, shown as x_2 in Fig. 6. This is determined by the following relation:

$$E_{I_2} = E_{O_1} - E_{R_1}. \quad (6)$$

where E_{I_2} is the injected energy of the second cycle and E_{R_1} the energy dissipated by the device during the first cycle. The stability of the system depends on the inherent damping of the device. The smaller the damping, the higher the risk of the system diverging. In order to stabilize the system and to reduce overshoot, a feedforward force offset is added to the driving force during the pressing path of every cycle

$$f_s = \begin{cases} K_p(x_m - x_s) + \Delta O, & \text{for} \quad \Delta(x_m - x_s) \geq 0 \\ K_p(x_m - x_s) - \Delta O, & \text{for} \quad \Delta(x_m - x_s) < 0 \end{cases} \quad (7)$$

where ΔO is the feedforward force offset which is updated every cycle and K_p is the proportional gain. Due to the addition of this feedforward force offset and with an analogous argumentation to (4), the condition specified in (6) will be met at a smaller overshoot,x_3 (see Fig. 7),when compared to the overshoot without offset, x_2 (see Fig. 6).

B. Estimation of Feedforward Force Offset

Estimating the correct value of the feedforward offset is important. Too small values of the offset may not allow

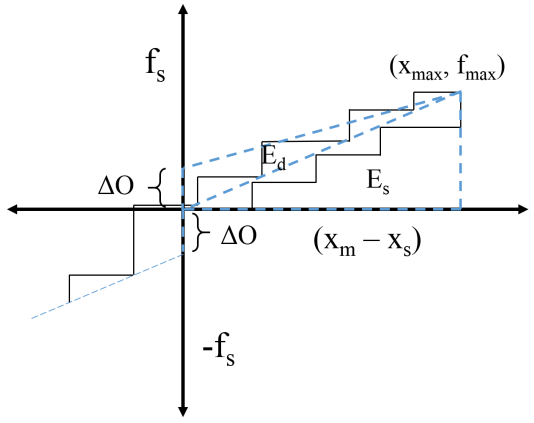

Fig. 8: Computing the value of feedforward force offset.

convergence of the system and too large values may result in a large force, which may cause sudden jerks that can damage the hardware. To make the proposed slave motion controller robust and independent from system parameters, we neglect the energy dissipated due to inherent damping of the device. This means we consider that the system is only allowed to overshoot until $E_{I_2} = E_{O_1}$.

If this were an analog system, then the energy E_S generated due to the motion of the slave and as illustrated in Fig. 8, would be:

$$E_S = \frac{x_{max} f_{max}}{2}. \tag{8}$$

where x_{max} is the maximum positional error which can be acquired from the device and f_{max} is the corresponding slave force.

However, since the system is not analog but discrete, there is some extra energy E_D generated due to the motion of the slave, see Fig 8:

$$E_D = \frac{\Delta O x_{max}}{2}. \tag{9}$$

At the end of every cycle, the output energy (E_O) can be determined from the system. It can be split into two components, the energy due to motion of the slave (E_S) and the generated energy due to the discrete interface (E_D):

$$\begin{aligned} E_O &= E_S + E_D, \\ E_O &= \frac{x_{max} f_{max}}{2} + \frac{\Delta O x_{max}}{2}, \\ &\quad rearranging, \\ \Delta O &= \frac{2}{x_{max}} \left(E_O - \frac{x_{max} f_{max}}{2} \right). \end{aligned} \tag{10}$$

Plugging the offset obtained by (10) into (7) results in

$$\begin{aligned} E_O(n-1) &= E_I(n) \\ &= \Delta T \sum_{k=0}^{n} (f_s(k) + \Delta O)(\dot{x}_m(k) - \dot{x}_s(k)). \end{aligned} \tag{11}$$

It is evident from (11) that larger ΔO results in smaller overshoot x_3, since $E_I(n) = E_O(n-1)$ for a smaller

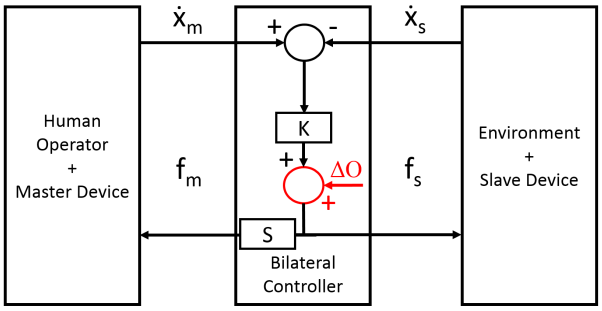

Fig. 9: Block diagram of a teleoperation system with the proposed SSI approach.

bouncing ($\sum_{k=1}^{n} (\Delta x_m(k) - \Delta x_s(k))$). This will make the injected energy of the current cycle equal to the released energy of the previous cycle at a smaller position error guaranteeing stable and fast convergence of the slave robot even for high controller gains. Fig. 9 shows the block diagram of a teleoperation system implementing the proposed SSI approach which increases the bandwidth of the slave robot while stabilizing the bilateral teleoperation for high gains. Here, S is a scaling factor.

Fig. 10: The experimental teleoperation setup consisting of two Phantom Premium 1.5 robots.

IV. Experimental Evaluation

In this section, experimental results for the proposed control method are reported.

A. Experimental Setup

The experimental setup is shown in Fig. 10. Two 3-DOF Phantom Premium 1.5 robots are connected via a latency-free communication channel. These devices offer negligible impedance and no resistive forces to the user conveying an almost perfect illusion of free space. A position-force control teleoperation architecture [13], [14], [15], with a PD motion controller ($P_s = 0.4$ kN/m, $D_s = 0.4$ kNs/m) has been implemented at slave side. In addition, the scaling factor $S = -1$ is chosen.

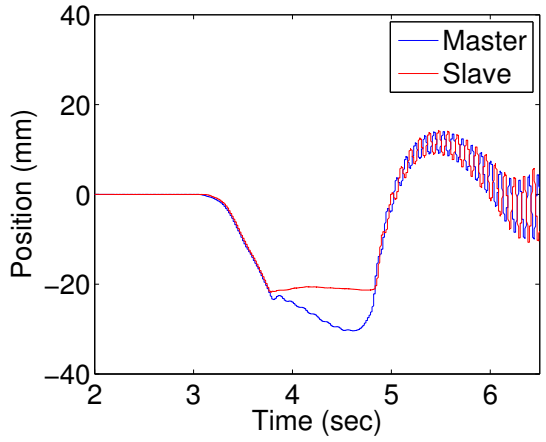

(a)

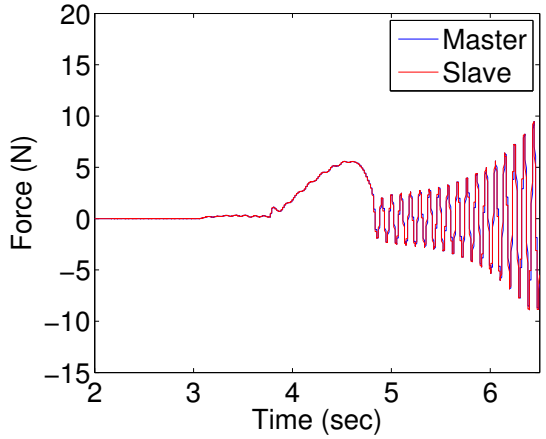

(b)

Fig. 11: Unstable (a) position and (b) force response of the teleoperation system with classical motion controller.

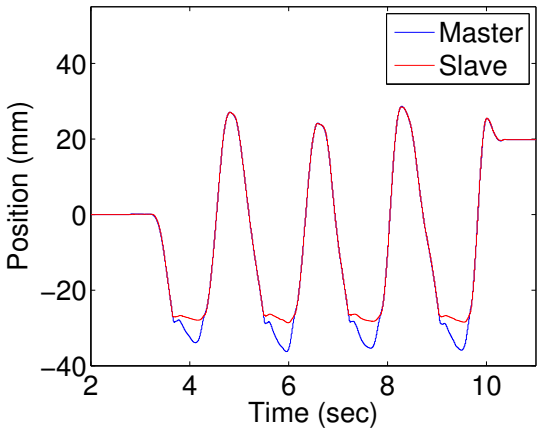

(a)

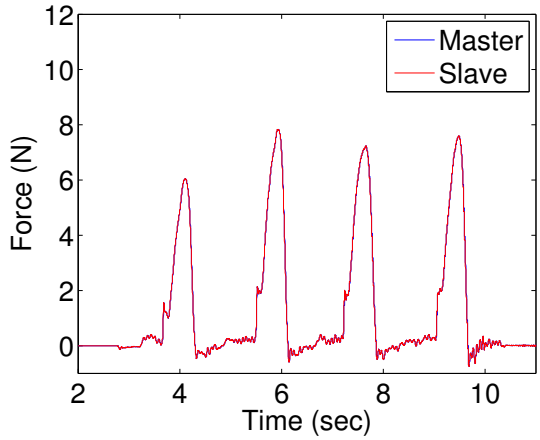

(b)

Fig. 13: Stable (a) position and (b) force response of the teleoperation system with the SSI approach.

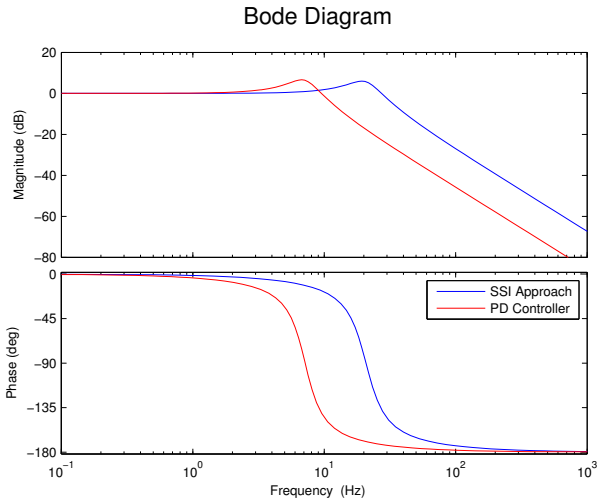

Fig. 12: Frequency response of the Phantom premium 1.5 for best tuned classical motion controller and SSI approach.

B. Experiment Results

Due to the feasibility of 2-channel position-force control architectures, the proposed SSI approach is exended based on a 2-channel position-force architecture. Therefore, a comparison of the performance of the proposed control architecture is compared with a 2-channel position-force control architcture. Note that 4-channel control architectures for tele-operation systems was out of the scope of this paper, however, one can easily interpret that compared to a 4-channel control architecture, the proposed control architecture is more practical not only because of its feasibility, but also due to the fact that 4-channel control architecture is more capable of becoming unstable when high gains are introduced.

Fig. 11 shows the position and force response of the system with the user interacting with a stiff remote environment at $x = -20$ mm, without any communication delay. The system is stable for $P_s = 0.4$ kN/m and $D_s = 0.4$ kNs/m. However, upon increasing the P gain ($P_s = 0.6$ kN/m), the position and force responses become unstable as soon as the user makes contact with a hard obstacle. This unstable behavior originates from the fact that the intrinsic damping of the slave robot is not large enough to dissipate the generated energy of the discrete bilateral controller. Thus, we cannot increase the bandwidth of the slave robot any further. The

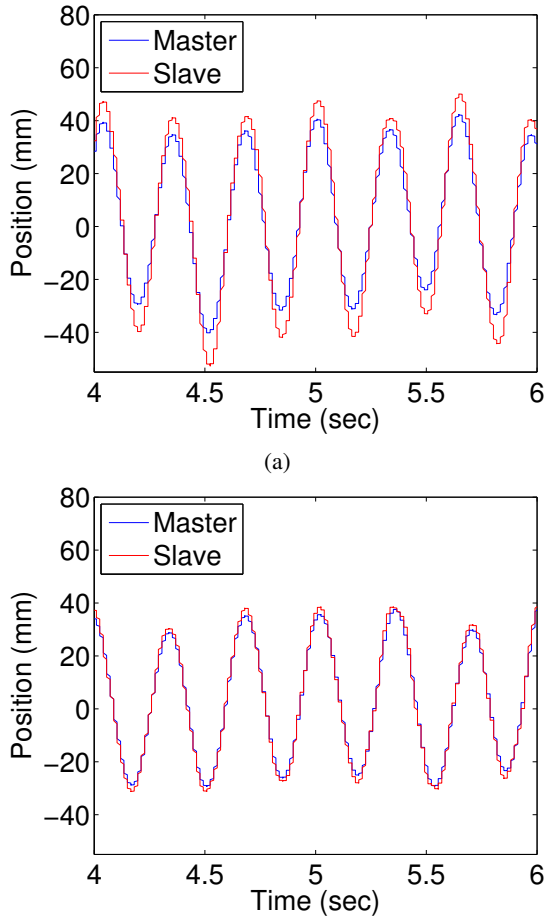

Fig. 14: Tracking performance of (a) best tuned classical motion controller and (b) SSI approach.

bandwidth of the slave robot for stable bilateral teleoperation is around 10 Hz, as can be seen from the recorded frequency response (Fig. 12). This is less than the bandwidth of the human arm, which is approximated to be around 20 Hz [10]. Thus, due to this bandwidth mismatch between human and slave robot arm, the user cannot fully exploit his/her manipulation capabilities.

Fig. 13 shows the experimental result of the proposed SSI approach with a high P gain ($P_s = 1.2$ kN/m), and without communication delay. The user makes repeated contacts with a remote obstacle located at x = -25 mm. The proposed approach adds a feedforward force offset to the control input. Thus, the injected energy equals the released energy of the previous cycle at a smaller position error, thereby reducing the overshoot. As can be observed the position error between master and slave decreases with each overshoot. This provides a sufficient condition for stable and fast convergence even for high P gains. Consequently, the force and position response (see Fig. 13) remain stable. It can be observed from Fig. 12 that the bandwidth of the slave robot increased to around 30 Hz which is more than the bandwidth of the human arm, while the conventional motion controller results in a bandwidth of 10 Hz. This allows the user to feel a sufficiently large interaction force with the remote environment without worrying about unstable behaviour and while using his/her full capability to control the slave robot.

Fig. 14 compares the tracking performance of the classical controller with that of the SSI approach when the user moves the master at high velocities. It can be seen that for the best-tuned classical controller ($P_s = 0.4$ kN/m and $D_s = 0.4$ kNs/m) the slave lags behind the master. This is not the case for SSI approach, where there is no visible delay between the motion of the master and slave. The classical controller also shows a larger overshoot than the SSI approach. Therefore, the SSI approach displayed better tracking performance compared to the classical motion controller.

V. Conclusion and Future work

In this paper, we extended the SSI approach to bilateral teleoperation systems for enlarging the bandwidth of the slave robot's motion controller. The main idea behind SSI approach is intentionally increasing one power conjugate signal in order to induce decrement of the other power conjugate signal following energy consistency. It is done by introducing a feedforward force offset which increases the feedback force and therefore decreases the position displacement. For bilateral teleoperation the power conjugate pair that defines the input/output energy relation was determined by position error and corresponding slave force. The pressing and releasing paths defined the injected and released energy to and from the system. We proposed the introduction of an adaptive feedforward force offset to the controller's output such that the injected energy during a cycle equals the released energy of the previous cycle at a smaller position error between master and slave. Experiments were conducted using a teleoperated pair of commercially available Phantom Premium 1.5. It was shown that using a best-tuned PD motion controller ($P_s = 0.4$ kN/m, $D_s = 0.4$ kNs/m) the teleoperation was stable. However, the bandwidth of the slave robot was about 10 Hz which is much smaller than that of a human arm (20 Hz). In order for the user to feel as if he/she were freely moving his/her own arm when manipulating the slave robot, it is very important for the human to be able to use his/her full bandwidth capabilities. This is only possible if there is no bandwidth mismatch between the user and slave robot arm. The SSI approach with high P gain ($P_s = 1.2$ kN/m) was able to keep the position and force response stable. This high gain also increased the bandwidth of the slave to around 30 Hz. Experiments conducted for high speed slave tracking showed that the stabilized system had a better tracking performance with smaller overshoot compared to the classical motion controller.

In this paper, we assumed that there is no time delay in the communication channel. However, this assumption may not be true for some applications. Thus, as a future work, we aim at investigating interaction cycles in communication channels to extend the SSI approach for time-delayed teleoperation systems.

ACKNOWLEDGMENT

This paper is partially supported by the Industrial Strategic Technology Development Program (10052967) funded by the Ministry of Trade, Industry & Energy (MOTIE), Korea.

REFERENCES

[1] Septimiu E Salcudean. Control for teleoperation and haptic interfaces. In *Control problems in robotics and automation*, pages 51–66. Springer, 1998.

[2] Peter F Hokayem and Mark W Spong. Bilateral teleoperation: An historical survey. *Automatica*, 42(12):2035–2057, 2006.

[3] Sandra Hirche, Manuel Ferre, Jordi Barrio, Claudio Melchiorri, and Martin Buss. Bilateral control architectures for telerobotics. In *Advances in Telerobotics*, pages 163–176. Springer, 2007.

[4] Jee-Hwan Ryu, Dong-Soo Kwon, and Blake Hannaford. Stable teleoperation with time-domain passivity control. *IEEE Transactions on robotics and automation*, 20(2):365–373, 2004.

[5] Changhoon Seo, Jaeha Kim, Jong-Phil Kim, Joo Hong Yoon, and Jeha Ryu. Stable bilateral teleoperation using the energy-bounding algorithm: Basic idea and feasibility tests. In *2008 IEEE/ASME International Conference on Advanced Intelligent Mechatronics*, pages 335–340. IEEE, 2008.

[6] FB Llewellyn. Some fundamental properties of transmission systems. *Proceedings of the IRE*, 40(3):271–283, 1952.

[7] Steven D Eppinger and Warren P Seering. On dynamic models of robot force control. 1986.

[8] Steven Eppinger and WARRENP Seering. Understanding bandwidth limitations in robot force control. In *Robotics and Automation. Proceedings. 1987 IEEE International Conference on*, volume 4, pages 904–909. IEEE, 1987.

[9] Edward Colgate and Neville Hogan. An analysis of contact instability in terms of passive physical equivalents. In *Robotics and Automation, 1989. Proceedings., 1989 IEEE International Conference on*, pages 404–409. IEEE, 1989.

[10] Michael J Fu and Murat Cenk Cavusoglu. Three-dimensional human arm and hand dynamics and variability model for a stylus-based haptic interface. In *ICRA*, pages 1339–1346, 2010.

[11] Harsimran Singh, Aghil Jafari, and Jee-Hwan Ryu. *Successive Stiffness Increment Approach for High Stiffness Haptic Interaction*, pages 261–270. Springer International Publishing, Cham, 2016.

[12] J Edward Colgate, Michael C Stanley, and Justin M Brown. Issues in the haptic display of tool use. In *Intelligent Robots and Systems 95.'Human Robot Interaction and Cooperative Robots', Proceedings. 1995 IEEE/RSJ International Conference on*, volume 3, pages 140–145. IEEE, 1995.

[13] M. Handlykken and T. Turner. Control system analysis and synthesis for a six degree-of-freedom universal force-reflecting hand controller. In *Decision and Control including the Symposium on Adaptive Processes, 1980 19th IEEE Conference on*, pages 1197–1205, Dec 1980.

[14] B. Hannaford and R. Anderson. Experimental and simulation studies of hard contact in force reflecting teleoperation. In *Robotics and Automation, 1988. Proceedings., 1988 IEEE International Conference on*, pages 584–589 vol.1, Apr 1988.

[15] Gary MH Leung, Bruce A Francis, and Jacob Apkarian. Bilateral controller for teleoperators with time delay via μ-synthesis. *IEEE Transactions on Robotics and Automation*, 11(1):105–116, 1995.